frontiers

The influence of clamping, structure geometry and material on seismic metamaterial performance

T. Venkatesh Varma [1], **Bogdan Ungureanu** [2,*], **Saikat Sarkar** [1], **Richard Craster** [2,3,4] **Sébastien Guenneau** [4] **and Stéphane Brûlé** [5]

[1] *Discipline of Civil Engineering, Indian Institute of Technology, Indore, India*

[2] *Department of Mathematics, Imperial College London, London SW7 2AZ, United Kingdom*

[3] *Department of Mechanical Engineering, Imperial College London, London SW7 2AZ, United Kingdom*

[4] *UMI 2004 Abraham de Moivre-CNRS, Imperial College London, London SW7 2AZ, United Kingdom*

[5] *Aix Marseille Univ, CNRS, Centrale Marseille, Institut Fresnel, France*

Correspondence*:
Bogdan Ungureanu - 180 Queen's Gate, London SW7 2AZ, United Kingdom
b.ungureanu@imperial.ac.uk

1 MATERIAL PROPERTIES

For convenience we summarize the geometry and elastic properties of the micro-structures in the following tables.

Table 1. Geometry of the micro-structures

Types	Width/thickness (m)	Length (m)	Diameter (m)	Substitution ratio
Medium soil	3	3	-	-
Loose soil	3	3	-	-
Circular inclusion	-	-	1.128	0.445
Regular shaped sqaure inclusion	2	2	-	0.445
Notch shaped square inclusion	2.25	2.25	-	0.445
Labyrinthine like inclusion	0.2	7	-	0.445
4 gap split ring inclusion	-	-	Outer 1.28 Inner 0.6	0.445
2 gap split ring inclusion	-	-	Outer 1.383 Inner 0.8	0.445
Swiss roll 1	0.128	-	1.128	0.445
Swiss roll 2	0.03	-	1.128	0.15
Seismic resonant inclusion	-	-	0 - 1.311	0 - 0.6

Table 2. Material properties

Material	Elastic modulus (MPa)	Poisson's ratio	Density (kg/m3)
Medium soil	153	0.3	1800
Soft soil	96.5	0.33	1650
Very soft clay type 1	10	0.25	1400
Very soft clay type 2	5	0.35	1633
Steel	200.000	0.33	7850
Concrete	35.350	0.15	2400

2 ADDITIONAL EFFECTS OF CLAMPING AND STRUCTURE GEOMETRY

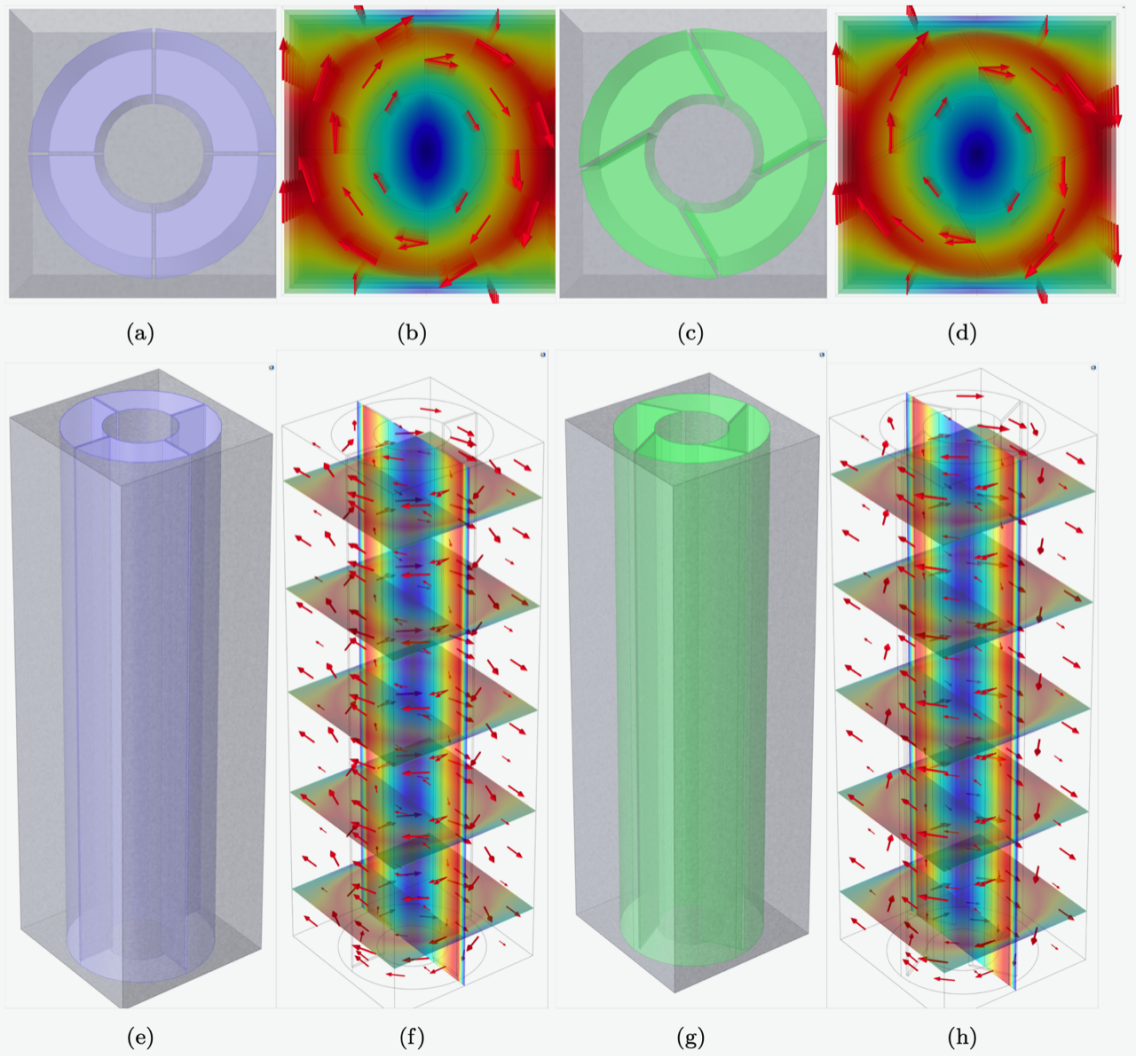

Figure 1. Unclamped cylindrical steel inclusion (radius $r = 0.62$ m, height $h = 10$ m) placed inside a cylindrical air cavity ($r = 1.3$ m, $h = 10$ m), surrounded by soil, inside an elementary cell (3 m $\times$3 m $\times$10 m) with periodic boundary conditions on opposite vertical sides, thus structuring soil in a doubly periodic manner. Each steel cylinder is connected to the soil matrix with 4 ligaments (0.04 m thick steel plates, 10 m in height). When ligaments are aligned with the center of the cell (a,e), a rotational eigenmode (b,f) occurs at frequency 42 Hz at high symmetry point M. When ligaments are tilted by an angle of 30 degrees with respect to the center of the cell (c,g), the rotational eigenmode (d,h) is shifted to frequency 38.6 Hz at high symmetry point M.

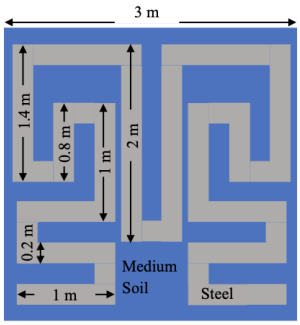

(a) Cross-section of cylindrical coil/Labyrinthine inclusion with substitution ratio 0.445

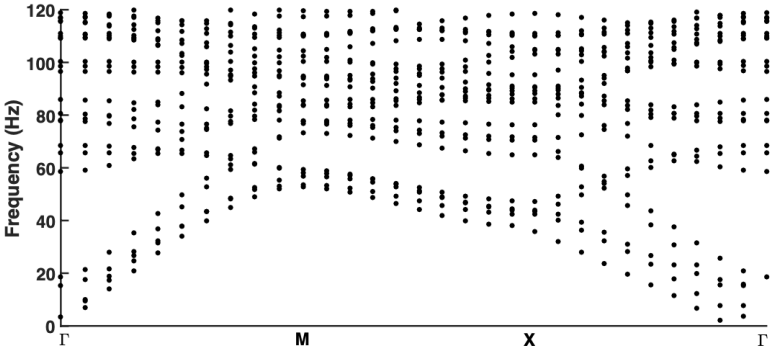

(b) Dispersion curves for cylindrical coil/Labyrinthine inclusion

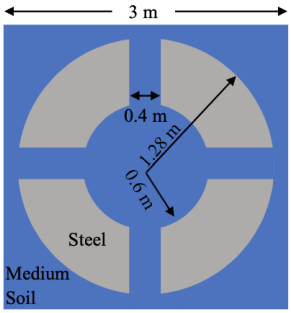

(c) Cross-section of 4 gaps cylindrical split-ring inclusion with substitution ratio 0.445

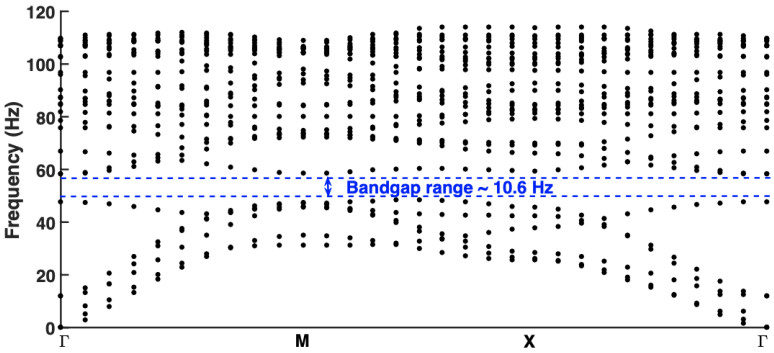

(d) Dispersion curves for 4 gaps cylindrical split-ring inclusion

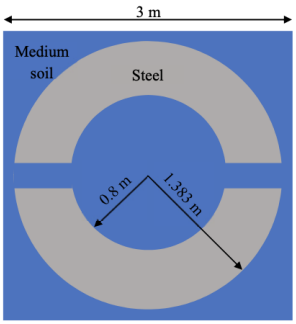

(e) Cross-section of 2 gaps cylindrical split-ring inclusion with substitution ratio 0.445

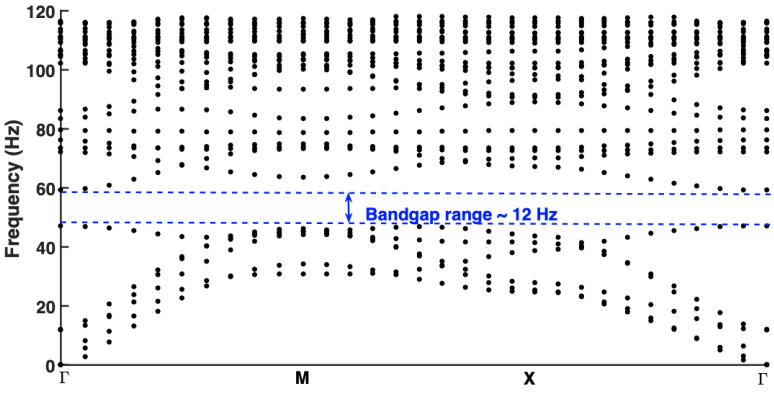

(f) Dispersion curves for 2 gaps cylindrical split-ring inclusion

Figure 2. Unclamped configuration of (a) coil/Labyrinthine, (c) 4 gaps split-ring and (e) 2 gaps split-ring with steel as inclusion with substitution ratio 0.445 in the elementary cell (3m x3m x10m) of periodic media (medium soil). Corresponding dispersion curves obtained around the edges of the irreducible Brillouin zone ΓXM are shown aside (b, d, f). Labyrinthine inclusion shows no bandgap in medium soil, whereas split-ring with same substitution ratio shows bandgap in the range of 45 Hz - 60 Hz. Notably, split-ring with 2 gaps shows an enhanced bandgap (12 Hz in the range of 46.84 Hz- 59.23 Hz) as compared to 4 gap split-ring (10.6 Hz in the range of 48.53 Hz- 58.35 Hz).

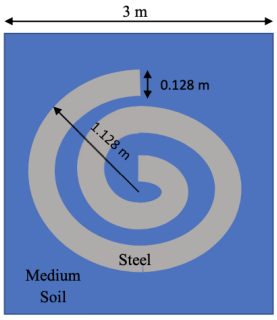

(a) Cross-section of cylindrical swiss roll-like inclusion with thickness 0.128 m

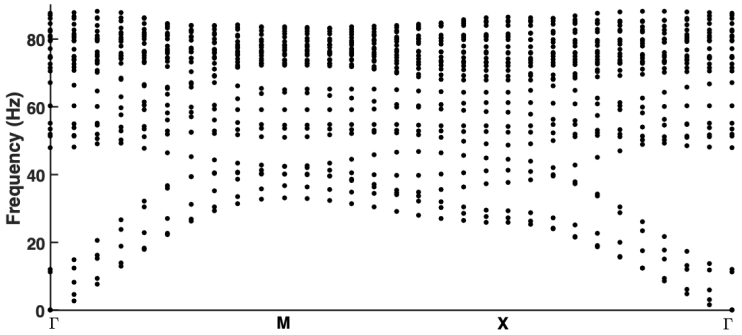

(b) Dispersion curves for cylindrical swiss roll inclusion with 0.128 m thickness

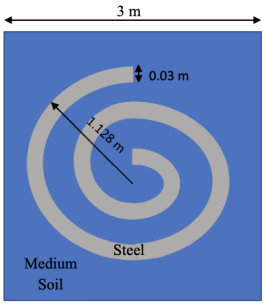

(c) Cross-section of cylindrical swiss roll inclusion with thickness 0.03 m

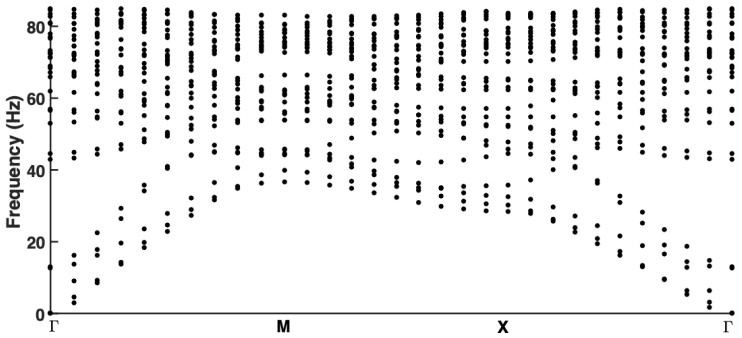

(d) Dispersion curves for cylindrical swiss roll-like inclusion with 0.03 m thickness

Figure 3. Unclamped configuration of cylindrical swiss roll like geometry with different thickness of steel inclusions in the elementary cell (3m x3m x10m) of periodic media (medium soil) . Diameter of swiss roll is considered same as solid circular inclusions in Fig.**??**. No bandgap is observed in both the cases

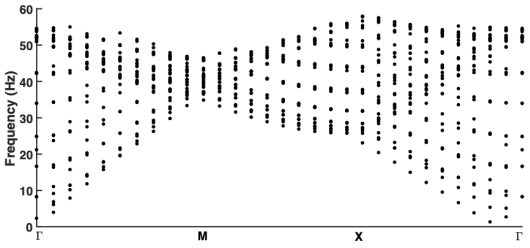

(a) Dispersion curve for Labyrithine microstructure with rubber as inclusion

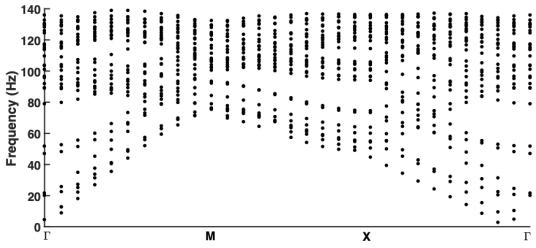

(b) Dispersion curve for Labyrithine microstructure with concrete as inclusion

Figure 4. Dispersion curves for unclamped configuration of Labyrinthine geometry as shown in fig. 4a with different constituent material, i.e., (a) rubber and (b) concrete. No bandgap is observed with these inclusions

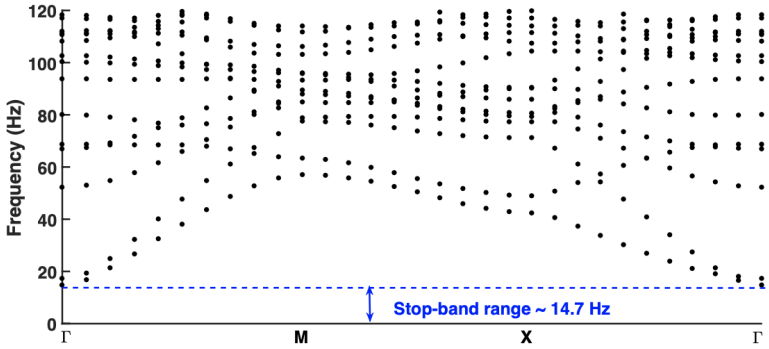

(a) Dispersion curves for cylindrical Labyrithine inclusion

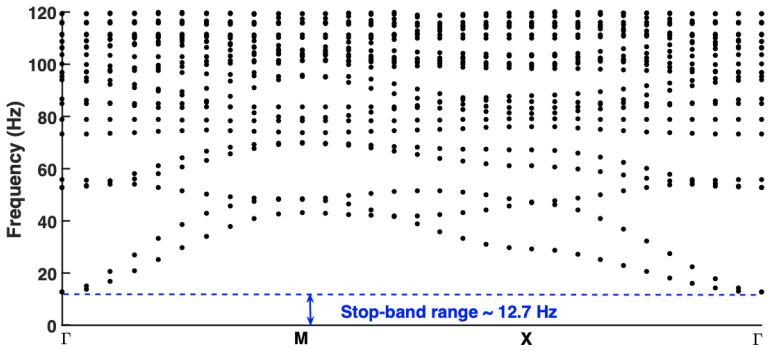

(b) Dispersion curves for cylindrical split-ring-like inclusion

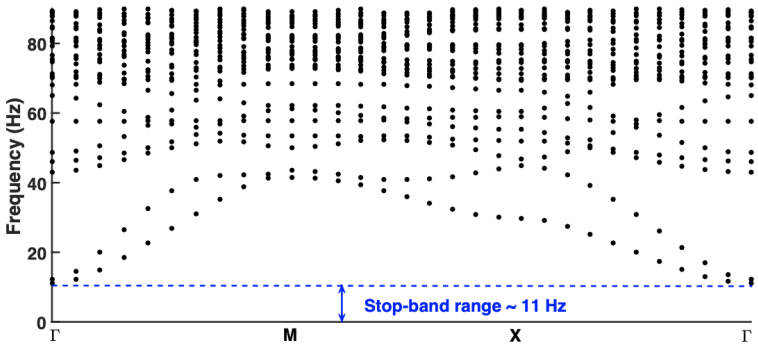

(c) Dispersion curves for cylindrical swiss-roll-like inclusion

Figure 5. Dispersion curves for clamped configuration with steel as inclusion material for (a) Labyrinthine, (b) 4 gaps split ring, and (c) swiss roll with 0.128 m thickness with substitution ratio as 0.445 (for swiss roll: 0.15).

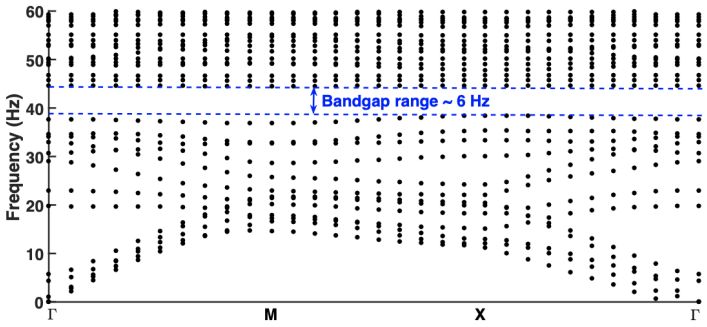

(a) Dispersion curves for cylindrical Labyrithine inclusion in very soft clay type 1 (cross-section details in Fig. 4a)

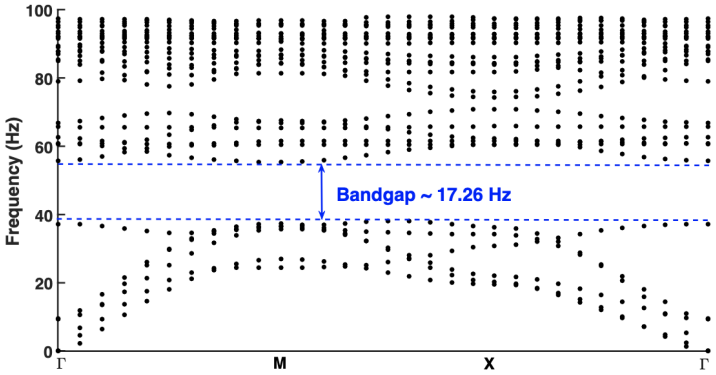

(b) Dispersion curves for 2 gap cylindrical split-ring-like inclusion in soft soil (cross-section details in Fig. 4e)

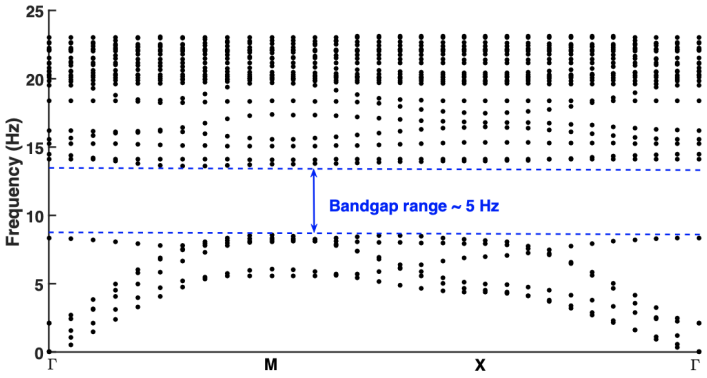

Figure 6. Dispersion curves for unclamped configurations of Labyrinthine and 2 gap split ring steel inclusions with 0.445 sustitution ratio in soft ($E = 96.5$ MPa, $\mu = 0.33$ and $\rho = 1650$ kg/m^3), very soft clay type 1 ($E = 10$ MPa, $\mu = 0.25$ and $\rho = 1400$ kg/m^3) and very soft clay type 2 ($E = 5$ MPa, $\mu = 0.35$ and $\rho = 1633$ kg/m^3) .

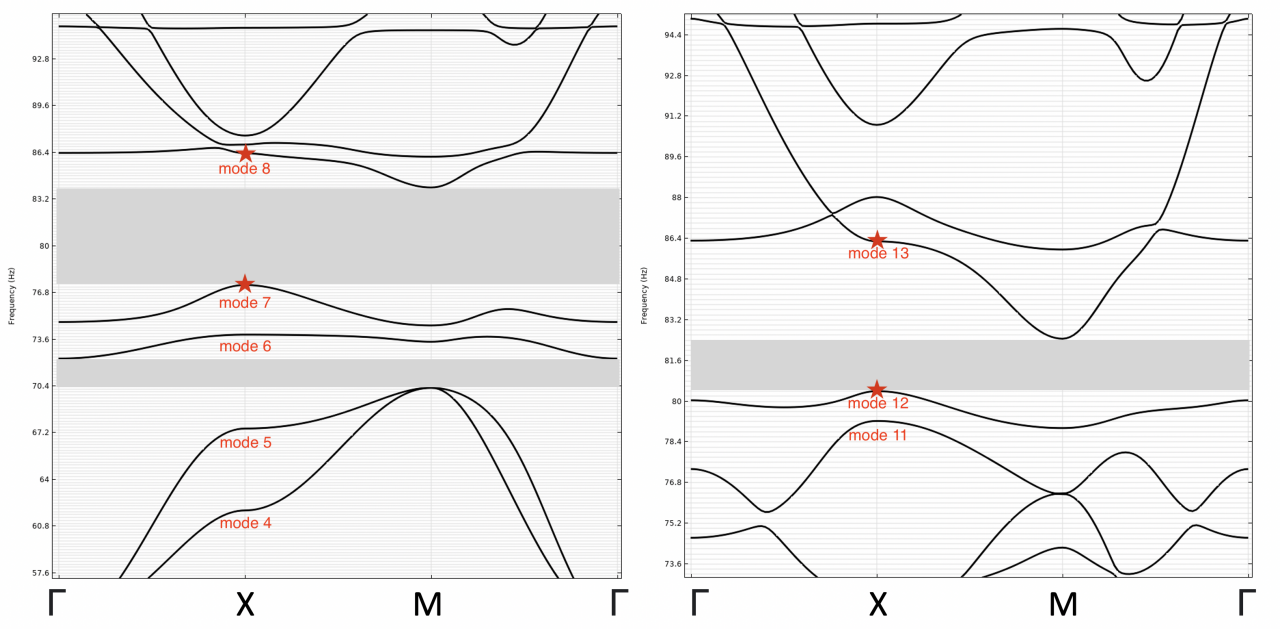

Figure 7. Zoom on the dispersion curves for clamped (left) and unclamped (right) cylindrical inclusions with 4 inclined ligaments corresponding to the Fig.**??**d respectively Fig.**??**b.

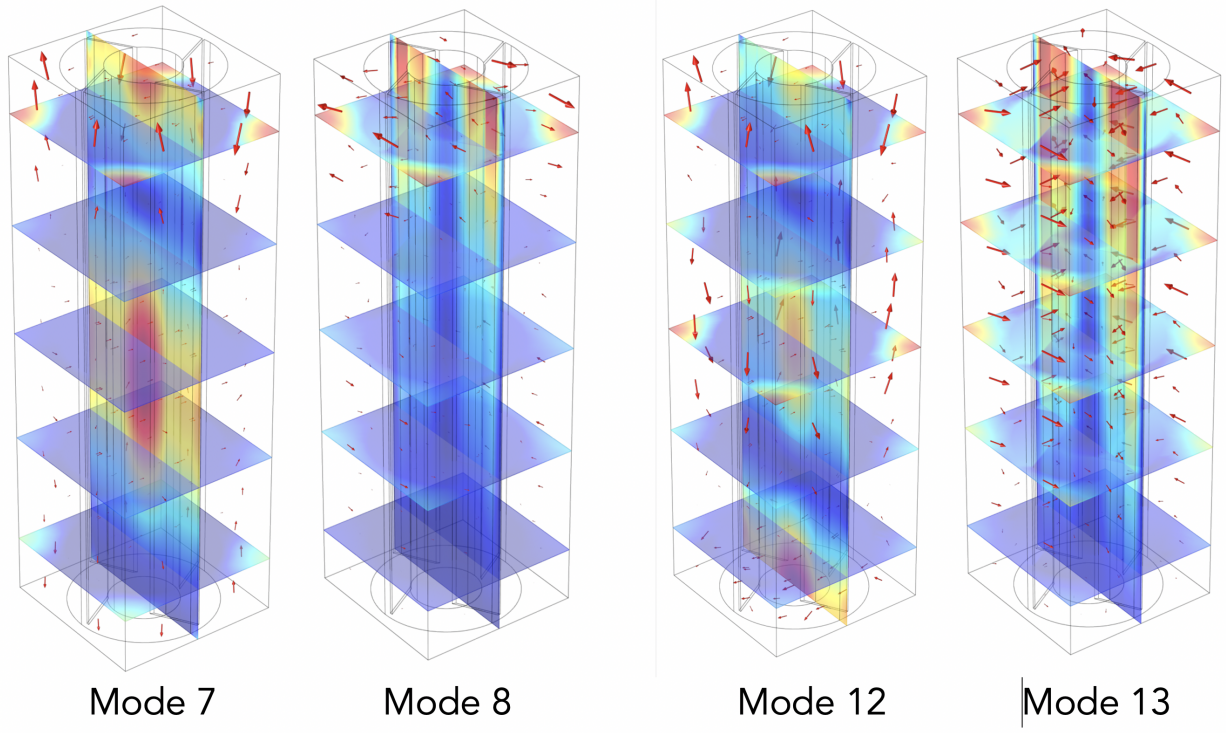

Figure 8. Representative eigenmodes for cylindrical inertial resonators (IRs) with 4 inclined ligaments at high-symmetry point X of the irreducible Brillouin zone $\Gamma X M$ corresponding to the star points in Fig.8: 7 and 12th modes are longitudial, 8th is torsional and 13 rotational.